



Exploring the Trend of Aerosol Optical Depth and its Implication on Urban Air Quality Using Multi-spectral Satellite Data During the Period from 2009 to 2020 over Dire Dawa, Ethiopia

Teshager Argaw Endale*† , Gelana Amente Raba*, Kassahun Ture Beketie** and Gudina Legese Feyisa**

*College of Natural and Computational Sciences, Department of Physics, Haramaya University, Dire Dawa, Ethiopia

**Center of Environmental Sciences, Addis Ababa University, Addis Ababa, Ethiopia

†Corresponding author: Teshager Argaw Endale; tesh.phy08@gmail.com; abnereth15@gmail.com

Nat. Env. & Poll. Tech.
Website: www.neptjournal.com

Received: 12-05-2023

Revised: 08-07-2023

Accepted: 01-08-2023

Key Words:

Atmospheric aerosol
Aerosol optical depth
Air quality
Model validation
Multi-spectral sensor

ABSTRACT

This study focuses on atmospheric aerosols, especially aerosol optical depth (AOD), over Dire Dawa, Ethiopia, from 2009 to 2020. At first, a correlation between the four satellite sensors and AERONET was made for validation purposes and to determine the sensor that best represents Dire Dawa. Intercomparisons were also made among the four satellite sensors. After all statistical tests, annual, seasonal, and decadal trend analyses were made. The validation results indicated that the AOD of MODIS-terra showed the best correlation with AERONET with R^2 (0.78), RMSE (0.03), and MBE of 0.02 and represented the area better than the rest. The inter-comparison of AOD retrieved from multi-spectral satellite sensors showed a positive and satisfactory correlation between MODIS-Terra and OMI. Only MODIS-Aqua showed a linearly increasing mean annual AOD with $R^2 = 0.43$. In three seasons (summer, autumn, and spring), AOD showed linear increments over the 12 years, with R^2 ranging between 0.3 and 0.5. The three seasons also had nearly identical AODs of 0.23-0.28. However, winter had the lowest value of 0.2. MODIS-terra, out of the four sensors, exhibited increasing decadal tendency over the 2009-2020 period. Monthly analysis revealed that August had the highest AOD (0.265), and January had the lowest (0.14). The value of AOD obtained from this study over Dire Dawa shows a higher value during all seasons except during winter. Thus, this study gives a glimpse into the use of multi-spectral satellite sensors to monitor air quality over a semi-arid urban region.

INTRODUCTION

Both natural and anthropogenic, atmospheric aerosols are amongst the major climate-forcing agents recognized globally (IPCC 2013). They play a major role in the Earth's climate system; weather, regional or global climate 'influence the Earth's radiation budget and affect the regional hydrological cycle (Ramanathan et al. 2001). Aerosols can both directly and indirectly change the radiation budget (Jung et al. 2019). Air quality is affected by aerosol. Aerosol dynamics in the atmosphere are closely correlated with regional meteorology and their emission sources. Aerosol ties alter throughout time and space as a result of their short lifetime and a number of dynamic processes, including transport, deposition, convection, and others. The high variation of aerosol properties poses significant challenges for comprehending aerosol observed by satellite remote sensing and modeling aerosol transport (Eck et al. 2008).

To some extent, the local air pollution level can be estimated using AOD, one of the basic optical metrics among aerosol properties. An exceedingly clean atmosphere has an AOD value of 0.01, whereas one that is quite cloudy has a value of 0.4. Aerosol is also widely utilized as an obscure but significant indicator of climate change and radiation equilibrium of the atmosphere (Wang et al. 2020, Weizhi et al. 2021). AOD exerts a great influence on climate regionally and globally since it affects atmospheric radiation, transmission, and water circulation (Rosenfeld et al. 2007). In the conventional sense, one way of AOD acquisition is by field exploration; this fails to meet the requirements of the regional study, and neither demonstrates spatial continuity. This is because of restrictions faced by the ground survey on allocating observation posts. Advancement in satellite remote-sensing techniques has opened new corridors for monitoring and mapping of air pollution over large regions. At present, remote sensing (R.S.) technology is a crucial mode for testing and supervising aerosol based on the

strength of AOD (Badarinath et al. 2011, Ge et al. 2011). Over the last decade, the Moderate Resolution Imaging Spectroradiometer is one example of a satellite sensor (MODIS) carried on both Aqua and Terra platforms (Levy et al. 2013), the Multiangle Imaging Spectroradiometer (MISR) and the Ozone Monitoring Instrument (OMI) (Levelt et al. 2006) have investigated the atmosphere by characterizing physical and chemical properties of aerosols using observations and retrieval algorithms.

Dire Dawa is the most vulnerable city to extreme climate events like drought, high flash floods, and high temperatures (Gezahegn et al. 2021). Frequent dust storms also occur in the area, especially during certain months of the year. Moreover, growing industrialization and expanding urbanization are contributing to more emissions of carbon monoxide, sulfates, and nitrates in the air (Oluwasinaayomi et al. 2018). Since no ground-based air-pollution monitoring instrument is available, the trend of AOD long-term data retrieved from multi-spectral satellite sensors. The present study has three main objectives. The first is to extensively evaluate MODIS Aqua, MODIS-Terra, MISR, and OMI satellites and to make an inter-comparison of the data obtained from the satellite sensors. This inter-comparison of multiple sensors is needed from time to time because errors and biases are present in retrieval algorithms due to instrument calibration, sampling, and algorithm accuracy. The second objective is to assess the temporal variation of AOD, i.e., decadal, seasonal, and annual variations over Dire Dawa. This helps to explore the magnitude and dispersion of AOD loading on the temporal scale in the study area. The third objective is to explore the AOD Mann-Kendall trend test. This study also attempted to identify the convenient satellite suitable for estimating AOD, which can reveal the status of air quality in a specific region, by inter-comparing AOD data sets retrieved from MODIS-Aqua, MODIS-Terra, MISR, and OMI with ground-based, AERONET, observations in Addis Ababa.

MATERIALS AND METHODS

Description of the Study Area

This study was carried out at the base of Dengego Mountain in Dire Dawa City, in the country's eastern region, 927° and 949°N latitude and 4138° and 4219°E longitude. Although the majority of the city is located at about 1200 m a.s.l., the height inside the city's boundaries spans from 960 m in the northeast to 2450 m in the southwest (Oluwasinaayomi et al. 2018). The average wind speed is about 2.67 m.s⁻¹, and relative humidity records indicate 49.13 ± 6.25. Dire Dawa is located about 515 km east of Addis Ababa, the capital city of Ethiopia, 55 km from Harar, and 313 km from Port of Djibouti. East Hararge administrative zone of Oromiya

Regional State borders Dire Dawa in the south and southeast and the Shinele zone of Somali Regional State in the north, east, and west. The major towns surrounding the city of Dire Dawa are Shinile, Gildessa, Hurso, Kulubi, Kombolcha, and Ejersa Goro. The total area of the Dire Dawa is about 128,802 ha. The city is a favored strategic position for both commercial and industrial activities. It is the main gateway for the country's trade route to Djibouti. The city is known for being an industrial and commercial center, comprising food-processing plants, textile and cement factories, and the second-largest open market in the country. In terms of population, Dire Dawa is the second biggest city in Ethiopia, next to Addis Ababa, with over 400,000 inhabitants (Oluwasinaayomi et al. 2018).

The high inflow of vehicles coupled with fast population growth has contributed to the problem of road traffic congestion (Belachew & Zeleke 2015). This is also the cause for the increase of air pollutants such as NO₂, CO₂, SO₂, CO, etc., which at some locations exceed the annual average level set in the ambient air quality standard (Knife, 2017).

The temperature trend indicates that the city exhibited a warming trend (Gezahegn et al. 2021). Oluwasinaayomi et al. (2018), analysis states that the maximum temperature has been rising at a rate of roughly 0.67°C per decade. The increase in land surface temperature appears to have been caused by a shift in land use and land cover due to urbanization, settlement development, and the building of additional homes in the city. Fig 1. depicts a map of the study region.

Satellite Data Processing and Analysis

Data sources: The data used in this study (AOD daily data from 2009 to 2020) were obtained from widely used satellite sensors for semi-arid regions, namely, MODIS Aqua, MODIS-Terra, MISR, and OMI except for MISR, which has only data available up to 2017. For validating the AOD data retrieved using the above sensors, the only available ground-based instrument, AERONET of Addis Ababa University, Ethiopia, was used. The description for each sensor was presented under sections 2.2.1, 2.2.2, 2.2.3, and 2.2.4, respectively.

MODIS-Aqua and MODIS-Terra: The moderate resolution imaging Spectro-radiometer (MODIS) is a remote sensing instrument on board by the National Aeronautics and Space Administration's (NASA's) Earth Observing Systems (EOS), Terra, and Aqua satellites launched in 1999 and 2002, respectively. MODIS operates at an altitude of 705 km and makes radiance observations in 36 spectral channels in the wavelength range of 410–1440 nm at a spatial resolution ranging from 250 m to 1 km with a 2300 km wide swath

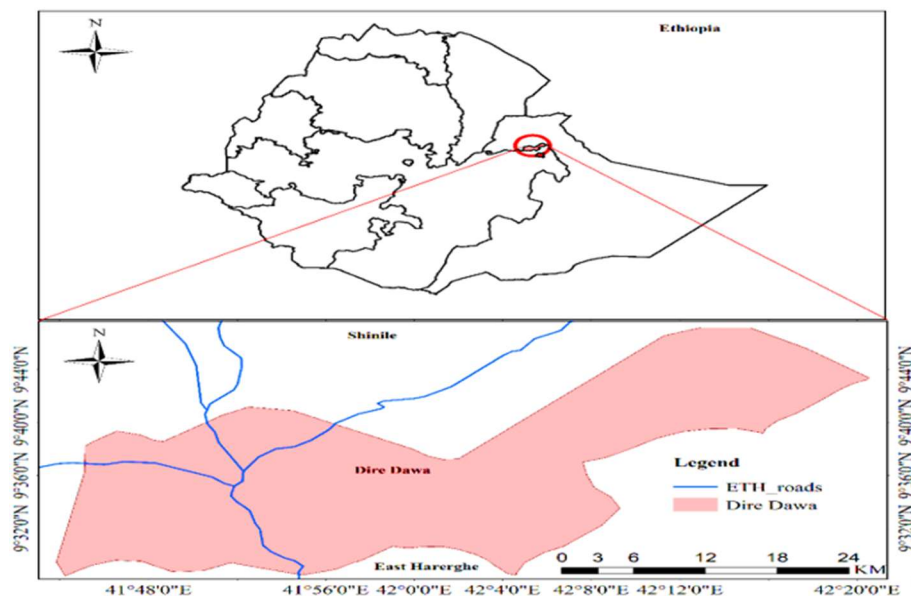


Fig. 1: Map of the study area of Dire Dawa.

and almost daily global coverage. Overland, MODIS AOD uncertainty is 0.05 ± 0.15 . Hsu et al. (2013) give MODIS aerosol retrieval details.

To retrieve aerosol optical properties (e.g., AOD information) over bright-reflecting surfaces such as desert and urban areas deep blue (D.B.) algorithm is used (Hsu et al. 2013). The blue channel is used since it provides low surface reflectance over the desert surface and can get the expected AOD information (Hsu et al. 2013). In this study, the website (<http://disc.sci.gsfc.nasa.gov/giovanni>) retrieved aerosol data from MODIS Aqua and Terra with collection 6, and a resolution of $1^\circ \times 1^\circ$ was used.

MISR data: The Multiangle Imaging Spectro Radiometer (MISR) instrument measures tropospheric aerosol characteristics through the acquisition of global multiangle imagery on the daylight side of Earth. MISR applies nine charge-coupled devices (CCDs), each with four independent line arrays positioned at nine view angles spread out at nadir, 26.1, 45.6, 60.0, and 70.5. In each of the nine MISR cameras, images are obtained from reflected and scattered sunlight in four bands – blue, green, red, and near-infrared – with a center wavelength value of 446, 558, 672, and 867 nm, respectively. The combination of viewing cameras and spectral wavelengths enables MISR to retrieve aerosols AOD over high-reflectivity surfaces like deserts.

In this study, we use Level 2 (version 0023) AOD at 558 nm (green band) measured by the MISR instrument with a 17.6 km resolution aboard the Terra satellite. The MISR data of $0.5^\circ \times 0.5^\circ$ has been rescaled by assigning equal

weight to each sub-grid, after which $1^\circ \times 1^\circ$ resolution was obtained. MISR Level 2 aerosol retrievals use only data that pass angle-to-angle smoothness and spatial correlation tests (Martonchik et al. 2002).

OMI data: OMI was launched in July 2004 on NASA's EOS-Aura satellite, which is also part of the A-train constellation. It has a nadir-viewing imaging spectrometer that measures the top of the atmosphere (TOA) upwelling radiances between the visible and ultraviolet solar spectrum (270–500 nm), with a spatial resolution of approximately 0.5 nm (Levelt et al. 2006). The expected uncertainty in AOD retrieval is around $\pm 30\%$ AOD or 0.10, whichever is more significant over Land (Ahn et al. 2014). This study utilized 500 nm observations with high-quality retrievals (Final Algorithm Flags = 0) from 2009 to 2020. The data was accessed from a website (<http://disc.sci.gsfc.nasa.gov/giovanni>).

AERONET data: AERONET is a well-organized, ground-based robotic network of more than 300 sites around the globe that uses a sky radiometer and sun photometer for aerosol measurements (Holben et al. 1998). The spectral ranges for the direct sun between 340–1020 nm and diffuse sky 440–1020 nm radiances are employed by a sun-photometer to take AERONET measurements. Ramachandran and Sumita (2013) reported that continuous data may be safely obtained from ground-based measurements of various aerosol characteristics over a particular location. In the present study, a level 1.5 sun photometer retrieved from AOD500 data from December 2020 to June 2021 was acquired from

AEROENT. The data was accessed from websites (<http://aeronet.gsfc.nasa.gov/>).

Data Validation

To validate AOD data retrieved from MODIS-Aqua, MODIS-Terra, and OMI, AERONET-AOD daily data from December 2020 to June 2021 were utilized. Analysis was performed based on data availability. Validation against AERONET and inter-comparison were made with the data of the three satellite sensors except for MISR, which did not have data from December 2020 to June 2021. The data was downloaded from the AERONET website (<http://aeronet.gsfc.nasa.gov/>). A summary of the sensors' wavelengths, product types, and resolutions is given in Table 1.

Procedure in Data Validation

Validation of satellite-derived AOD involves comparison with ground-based measurements. Such comparison helps in determining uncertainties in satellite measurements and the development of improved algorithms (Cheng et al. 2012). AOD data validation in the period from 2009 to 2020, we compared results obtained from MODIS-Aqua, MODIS-Terra, MISR, and OMI, with AERONET. Satellite sensors retrieve AOD at different wavelengths: MODIS at 470, 550, and 660 nm, MISR at 446, 558, 667, and 862 nm, and OMI at 342.5, 388.0, 442.0, 463.0, 483.5, and 500.0 nm. For increased accuracy in the validation, the AERONET-based AOD wavelength is interpolated logarithmically to each of the satellite-derived AOD using the Ångström power law. If AOD and Ångström exponent at one wavelength are known, then AOD at a different wavelength can be computed as:

$$AOD_a = AOD_b \left(\frac{a}{b}\right)^{-\alpha}$$

Variables a and b assume the values 550 nm and 555 nm for MISR and 500 nm (each) for OMI and AERONET, respectively. These wavelength ranges were selected since they are close to the average between the standard

wavelengths of various sensors (440 nm to 865 nm).

Statistical Techniques

In this study, after AOD data were retrieved using multi-spectral satellite sensors for 12 years (i.e., 2009 to 2020) a statistical test parameter such as linear regression: intercept, slope, R^2 (determination coefficient), and other statistical parameters such as MBE (mean bias), MAE (mean percentage error), Relative mean bias (RMB) and RMSE (root-mean-square), Mean absolute percentage error (MAPE) (Tripathi et al. 2005, Floutsi et al. 2016). The accuracy of each of the algorithms was further assessed using EE (Remer et al. 2005, Kristjánsson et al. 2014), defined as the confidence envelopes for each of the AOD retrieval algorithms.

The coefficient of the residual mean (CRM), Coefficient of Efficiency (C.E.), and a 1:1 line is required to see whether the regression line falls above, below, or if it crosses this line (Mengistu & Amente 2020). In addition, the Mann-Kendall non-parametric test (Taotao et al. 2016) was used to observe the temporal trends. All the necessary Mann-Kendall test parameters were determined along with Sen's slope using Python programming.

RESULTS AND DISCUSSION

Validation of AOD with AERONET and Intercomparisons of AOD Data of the Satellite Sensors

Validation of MODIS-Aqua, MODIS-Terra, MISR, and OMI over Dire Dawa

Ground-based observations are used to validate satellite aerosol products both globally and regionally. Daily AOD values of the four sensors were compared with ground-based interpolated AERONET-AOD for Dire Dawa during 2020-2021. Fig. 2 shows the regression results between daily-averaged AODs for MODIS-Aqua, MODIS-Terra, and OMI with AERONET at 550 nm.

As observed in Fig. 2, even if the AOD results of all three sensors showed a positive correlation with that of

Table 1: Summary of data sets (Satellite and ground observation) used for the study from 2009 to 2020.

Sensor	Product Type	Parameters	Resolution		Data used	Remark
			Temporal	Spatial		
MODIS-Aqua(550nm)	MYD08D3V6.1	AOD, D.B.	Daily	1°	2009-2020	
MODIS-Terra(550nm)	MOD08D3V6.1	AOD, D.B.	Daily	1°	2009-2020	
MISR (555nm)	MIL3DAEV4	AOD	Daily	0.5°	2009-2017	NDA beyond 2017
OMI (500nm)	OMAERUVdv003	AOD	Daily	1°	2009-2020	
AERONET (500nm)		AOD	Daily	1°	Dec.2020-June2021	NDA before 2020

NDA= No data available

AERONET, the best correlation was observed between MODIS-Terra and AERONET ($R^2 \sim 0.71$ for linear fit without intercept and 0.78 (for linear fit with intercept).

The linear fit between MODIS-Aqua and AERONET gave $R^2 \sim 0.52$ for both with and without intercept. Besides, all points fell within P.B. of 95% Confidence Interval (CI), and the slopes of all the plots are also close to 1. Tables 2a and 2b show the statistical accuracy of the linearly fitted (with and without intercept) for the three sensors.

As seen in Table 2a, all three sensors showed positive linear correlations with AERONET data. Out of the three, MODIS-Terra exhibited the best correlation with AERONET in terms of R^2 ($=0.78$), RMSE (0.03), good R^2 and slope, and MBE of 0.02. Overall, the AOD data of this sensor could be taken as the best representation of Dire Dawa AOD. Using curve fit without intercept, MODIS Terra again outperformed the rest since it exhibited the highest R^2 ($=0.72$) and E.E. (82.2%), good R^2 and slope, MBE close to zero (0.02), and the fit line is close to the 1:1 line with very slight overestimation. Previous research by Levy et al. (2010) identified a calibration problem with the MODIS

that would affect AOD time series analysis and reported some difficulties with the satellite-based AOD retrievals over Land. For instance, according to Levy et al. (2013), MODIS tends to overestimate AOD over bright land surfaces, including urban areas, relative to AERONET. In this respect, this paper also shows agreement with their studies since, despite the positive correlation, both MODIS sensors showed slight overestimation.

The close agreement of the two fitted lines (with and without intercept) indicates a good correlation between sensors' and AERONET data. Since the air distance between Addis Ababa (location of AERONET data) and Dire Dawa is not greater than 300 km, it is safe to use the AOD of the best sensor (which in this case is MODIS terra) to represent Dire Dawa's AOD.

As shown in Table 2b, by the 1:1 line, all three sensors showed slight overestimation since they are all above the 1:1 line). By CE, MODIS-Aqua was good; MODIS-Terra was satisfactory, and OMI demonstrated poor performance. However, the effectiveness of the model by R^2 and slope was satisfactory and good for both MODIS-Aqua and

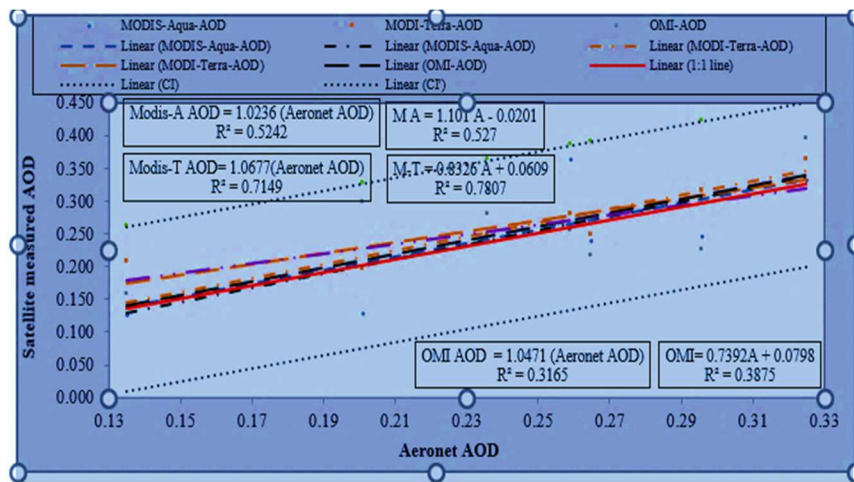


Fig. 2: Validation of AOD data retrieved from MODIS-Aqua, MODIS-Terra, and OMI sensors with AERONET over Dire Dawa. The linear curve fits were made with (right-side equations) and without intercepts (left-side equations).

Table 2a: Statistical parameters, model tendencies, and performance tests of the three AOD regression models over Dire Dawa (linear fits with intercepts).

A vs Sensor	Statistical parameters				Model tendency by			Model performance by					
	R^2	Slope	Intercept	RMSE	CRM	Slope (%)	1:1 line	CE	R^2 & slope	MBE	MAPE (%)	PB	
M-A vs A	0.527	1.101	0.020	0.06	CA (-0.02)	OE (10.1)	SOE	G (0.94)	S & G	SOE (0.005)	VG (9)	API	
M-T vs A	0.781	0.893	0.061	0.03	CA (-0.08)	UE (10.7)	SOE	S (0.69)	G & G	SOE (0.02)	VG (9.8)	API	
OMI vs A	0.388	1.047	0.080	0.05	SUE (0.9)	OE (26.1)	SOE	P (0.04)	S & G	SOE (0.02)	VG (8)	API	

A = AERONET, M-A = MODIS-Aqua, M-T = MODOS-Terra, CA = close agreement, SOE= slight overestimation), SUE = slight underestimation, U.E. = underestimation, S = satisfactory, G = Good, P = Poor, VG = very good, P.B. = 95% prediction bound, and API= All points included in P.B. Numbers in brackets under 'slope' represent the percent O.E. or U.E. while the ones under RMSE represent the percent error of AOD.

Table 2b: Statistical parameters, model tendencies, and performance tests of the three AOD regression models over Dire Dawa. (Linear fit without intercept).

A vs Sensor	Statistical parameters				Model tendency by			Model performance by				
	R ²	Slope	EE (%)	RMSE	CRM	Slope (%)	1:1 line	CE	R ² & slope	MBE	MAPE (%)	PB
M-A vs A	0.52	1.023	71.4	0.06	CA (-0.02)	OE (2.3)	SOE	G (0.94)	S&G	SOE (0.005)	VG (9)	API
M-T vs A	0.72	1.067	82.2	0.03	CA (-0.08)	OE (6.7)	SOE	S (0.69)	G&G	SOE (0.02)	VG (9.8)	API
OMI vs A	0.32	1.047	59.6	0.05	SUE (0.9)	OE (4.7)	SOE	P (0.04)	S&G	SOE (0.02)	VG (8)	API

A = AERONET, M-A = MODIS-Aqua, M-T = MODOS-Terra, CA = close agreement, SOE= slight overestimation), SUE = slight underestimation, U.E. = underestimation, S = satisfactory, G = Good, P = Poor, VG = very good, P.B. = 95% prediction bound, and API= All points included in P.B. Numbers in brackets under 'slope' represent the percent O.E. or U.E. while the ones under RMSE represent the percent error of AOD.

OMI sensors, whereas MODIS-Terra demonstrated good performance for both R² and slope. The RMSE statistical test indicator showed values (of 0.06, 0.03, 0.05) that are close to zero, but MODIS Terra exhibited the least value. The E.E. values are all 60% or more. Here again, MODIS-Terra showed a superior value of 82%, followed by MODIS-Aqua. A study by Ashraf (2018) on MODIS, MISR, and AERONET climatology comparison across the Middle East and North Africa showed the performance of MODIS to be similar over the entire region, with ~68% of AOD within the confidence range. In this study, all the points are almost within the confidence interval. Gupta et al. (2018) found that 62.5 and 68.4 % of AODs retrieved from Terra MODIS and Aqua MODIS, respectively, fall within previously published expected error bounds of $\pm (0.05 + 0.2 \times \text{AOD})$, with the coefficient of determination (R²) of ≥ 0.5 , which is in agreement with this study. In the study by Bibi (2015) where they made intercomparisons of MODIS, MISR, OMI, and validation against AERONET, they obtained results similar

to this study. The study of Kazuhisa et al. (2022) revealed that the localized uncertainties, particularly surrounding a humid coastal city, are exacerbated by heterogeneous surface reflectance, mixed aerosol optical characteristics, and strong meteorological variability, and as Dire Dawa is located in such a location this might affect the variation of AOD retrieval among the sensors.

Inter-comparison of MODIS-Aqua, MODIS-Terra, MISR, and OMI

Fig. 3(a) shows the inter-comparisons of data sets retrieved over Dire Dawa by the four sensors from 2009 to 2020.

As shown in Fig. 3a – 3f, the linear curve fits are done with intercepts (dashed lines) and without intercepts (solid lines). Considering the linear curve with intercepts, none (except the fit between MODIS T and OMI) gave even satisfactory correlations, as seen from the R² values. However, the slopes can be considered good. The tabular values of model tendencies and performance

Table 3a: Statistical parameters, model tendencies, and performance tests of the three AOD regression models over Dire Dawa for the linear fit with intercept.

Correlation	Statistical parameters				Model tendency by			Model performance by				
	R ²	Slope	Intercept	RMSE	CRM	Slope [%]	1:1 line	MBE	CE	R ² & slope	MAPE [%]	PB
M-A vs M-T	0.24	0.347	0.148	0.068	UE(0.02)	U.E. (65.3)	Mixed	UE(-0.02)	S (0.38)	P & P	G (19.96)	MPI
M-A vs OMI	0.14	0.335	0.174	0.081	OE(-0.06)	U.E. (66.5)	Mixed	UE(-0.05)	P (-0.15)	P & P	S (30.94)	MPI
M-A vs MISR	0.07	0.238	0.183	0.151	OE(-0.03)	U.E. (76.2)	Mixed	O.E. (0.19)	P (-0.24)	P & P	G (13.79)	MPI
M-T vs OMI	0.33	0.719	0.088	0.060	OE(-0.09)	U.E. (28.1)	Mixed	UE(-0.02)	G (0.95)	S & G	G (19.78)	MPI
M-T vs MISR	0.04	0.299	0.173	0.147	UE(0.2)	U.E. (70.1)	Mixed	OE(0.05)	G (0.93)	P & P	S (21.82)	MPI
OMI vs MISR	0.02	0.156	0.200	0.159	OE(-0.02)	U.E. (84.4)	Mixed	UE(-0.07)	P (-0.88)	P & P	S (24.54)	MPI

M-A = MODIS-Aqua, M-T = MODOS-Terra, SUE = slight underestimation, P.O. = perfect overlap, SO = slight overlap, O.E. = overestimation, SOE = slight overestimation, MPI = most points included in P.B.

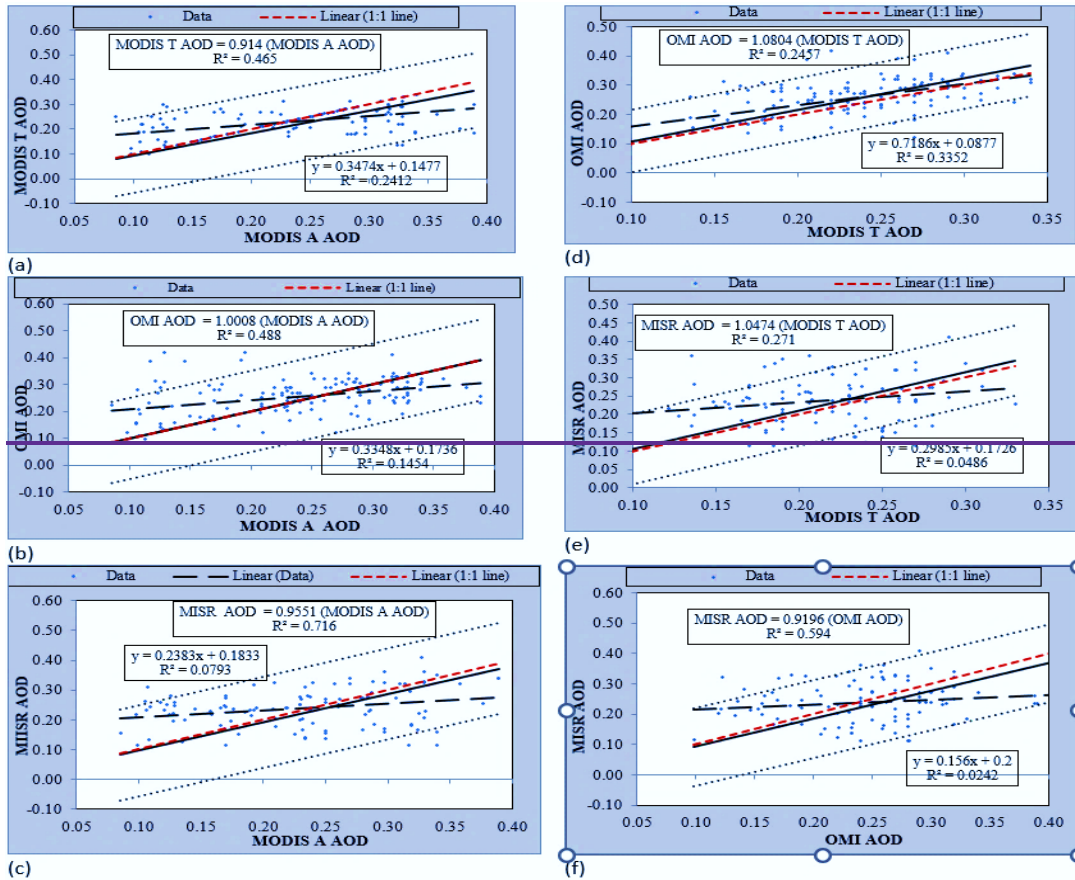


Fig. 3: Comparisons between (a) MODIS-Aqua vs MODIS-Terra, (b) MODIS-Aqua vs OMI, (c) MODIS-Aqua vs MISR, (d) MODIS-Terra vs OMI, (e) MODIS-Terra vs MISR (f) OMI vs MISR. The linear fit equation with and without intercept and coefficient of determination (R^2) are also given.

Table 3b: Statistical parameters, model tendencies, and performance tests of the three AOD regression models over Dire Dawa for fit line without intercept.

Correlation	Statistical parameters			Model tendency by			Model performance by				
	R^2	Slope	RMSE	CRM	Slope [%]	1:1 line	MBE	CE	R^2 & slope	MAPE [%]	PB
M-A vs M-T	0.465	0.914	0.068	UE(0.02)	UE (8.6)	SUE	UE(-0.02)	S (0.38)	S & G	G (19.96)	MPI
M-A vs OMI	0.488	1.001	0.081	OE(-0.06)	O.E. (0.1)	P.O.	UE(-0.05)	P (-0.15)	S & G	S (30.94)	MPI
M-A vs MISR	0.716	0.955	0.151	OE(-0.03)	UE (4.5)	SO	OE (0.19)	P (-0.24)	G & G	G (13.79)	MPI
M-T vs OMI	0.246	1.080	0.060	OE(-0.09)	O.E. (8.0)	O.E.	UE(-0.02)	G (0.95)	P & G	G (19.78)	MPI
M-T vs MISR	0.271	1.047	0.147	UE(0.28)	OE (4.7)	SOE	OE(0.05)	G (0.93)	P & G	S (21.82)	MPI
OMI vs MISR	0.594	0.920	0.159	OE(-0.02)	U.E. (8.0)	SUE	UE(-0.07)	P (-0.88)	S & G	S (24.54)	MPI

M-A = MODIS-Aqua, M-T = MODOS-Terra, SUE = slight underestimation, PO = perfect overlap, SO = slight overlap, OE = overestimation, SOE = slight overestimation, MPI = most points included in PB

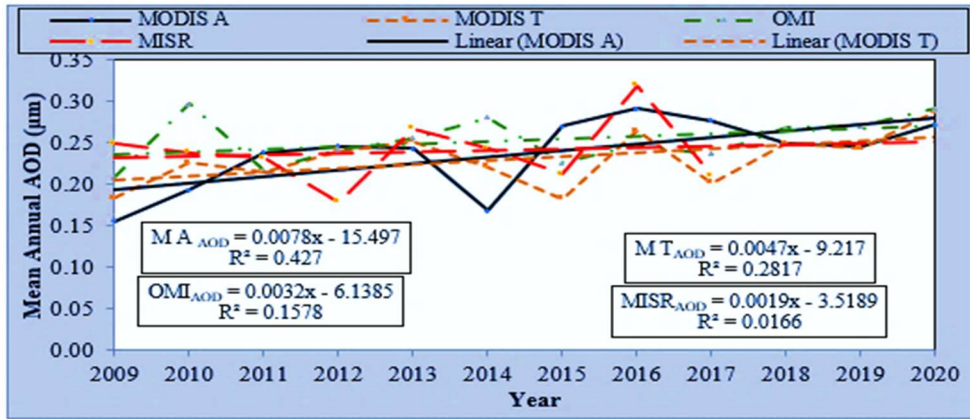


Fig. 4: Annual distribution of AOD retrieved using MODIS-Aqua (M A), MODIS-Terra (M T), OMI, and MISR from 2009 to 2020.

tests for the fitted line with intercept are shown in Table 3a.

The study of Ashraf (2019) revealed that Both MISR and MODIS provide a decent representation of the AOD climatology, in the Middle East and North Africa. Moreover, the study of Kazuhisa et al. (2022) revealed that the localized uncertainties, particularly surrounding a humid coastal city,

are exacerbated by heterogeneous surface reflectance, mixed aerosol optical characteristics, and strong meteorological variability. As Dire Dawa is located in such a location, this might affect the variation of AOD retrieval among the sensors.

The fit line without intercept (though not as effective as the one with intercept) can show us the nature of the

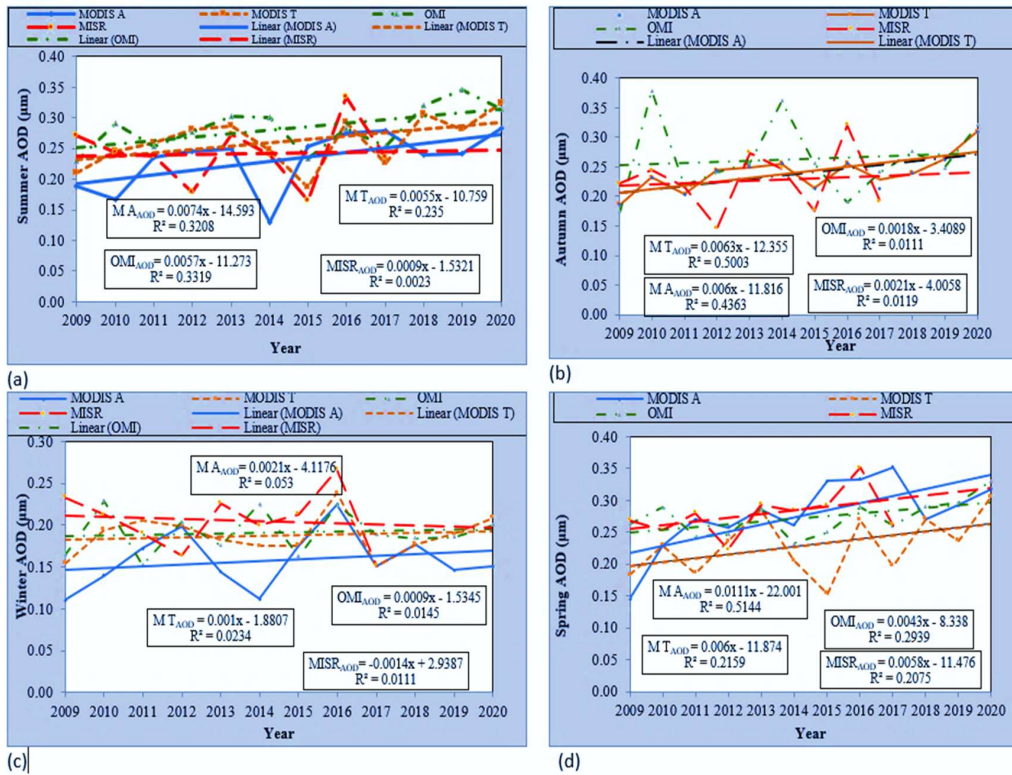


Fig. 5: Seasonal AOD retrieved from MODIS-Aqua, MODIS-Terra, MISR, and OMI in (a) summer, (b) autumn, (c) winter, and (d) spring seasons for the period of 2009 to 2020 over Dire Dawa.

correlations, as shown in Table 3b. In this case, there is no crossing of the fit line and the 1:1 line since the fit line is forced to pass through the origin (0, 0) point. This makes all the slopes within the acceptable limit and four out of the six R^2 values in the satisfactory range. The 95% prediction bound (P.B.) is shown in all the figures for this fit line, indicating most of the data points included within the bound. In this case, best fits were obtained between MODIS-Aqua and MISR AOD. However, this curve fit hides the correct tendency and nature of the correlation between the data points of the sensors.

Trend Analysis of AOD Data

Annual Variability of AOD Over Dire Dawa

The long-term linear AOD trend analysis was made using MODIS-Aqua, MODIS-Terra, OMI, and MISR over Dire Dawa from 2009 to 2020. The results are shown in Fig. 4.

In the figure, all the results revealed linearly increasing trends, though only that of MODIS aqua seems to have a satisfactory positive correlation. Such a positive trend of MODIS aqua exhibits a change in aerosol concentration of approximately 0.78% per year, which is the value of the slope of the MODIS_Terra equation. That of MODIS Terra comes to 0.47% per year. The difference between the two is 0.31%. Taking the value of MODIS terra as a representative for Dire Dawa, it takes around 40 years to double the current value of AOD of 0.20.

Ashraf (2019), in his study of dust-dominated sites in China, observed positive trends between MODIS-Terra, MODIS-Aqua, and MISR, unlike the weak correlations observed in this study. Based on these studies, highly concentrated aerosols in a certain region may indicate the occurrence of secondary particles resulting from industrial and urban pollutants, as well as biomass burning from various agricultural activities. In Dire Dawa, the increasing annual trend is not vivid at this time, perhaps due to the buffering effect of the surroundings or the offsetting effect of one season by another.

Seasonal Variability of AOD Over Dire Dawa

To see the yearly variability of AOD, seasonal differences were determined by dividing the year into four seasons, namely, summer (June - August), autumn (September - November), Winter (December - February), and spring (March-May). Using the data of a specific season and plotting the trends over 12 years helps to visualize the change season-wise. The plots of each season are shown in Figs. 5a-5d.

Three of the four sensors (M A, M T, and OMI) data showed slightly positive AOD trends during the summer season over the twelve years. The linear fits are satisfactory

for M A and OMI. This season is one of the rainy seasons for the area and is therefore marked by increased water vapor and cloud cover in the atmosphere. The precipitation cleans the atmosphere and is responsible for reducing the AOD in the air. Despite that, the increase is by 0.74%/y for M A and 0.57%/y for OMI, which is close to the value of M T (0.53%/yr). The increase in AOD concentration over the years for this season may indicate a change in climates, such as a decline in rainfall, or it can be linked with increased urbanization, industrial expansion, and the like. Both MODIS sensors indicated satisfactory increasing trends for autumn, with 0.6%/y for M A and 0.63% for M T. The result, in this case, is close to that of the summer season.

None of the sensors' data depicted any trend in winter. Winter is when the atmosphere is clear (no clouds, no precipitation, and very small water vapor in the atmosphere). The temperature is relatively cooler, and the wind is also calmer. Despite changes such as increased land use/cover over the 12 years, the fact that AOD concentration remained constant during this season over the 12 years indicates that there is something that offsets the increment.

Increasing temperatures cause the local wind to produce thermal variations because of unequal heating, and the temperature difference leads to increased turbulence. The cooler temperature, calmer wind, and the lack of pollens (dormancy time of plants) in the winter decrease the number of aerosol particles that get into the atmosphere. Even the few particles that are airborne experience limited upward movement because of a lack of turbulence in the atmosphere. Besides, these particles take less time to return to the ground. These reasons seem to be the causes for the reduced AOD in the winter.

Almost all of the sensors indicated linearly increasing AOD trends over the 12 years for the spring season. The fits are satisfactory for M A with an increment of 1.11%/y and almost satisfactory for M T with a trend of 0.43%/y. Spring is a windy time and is also known for its short rainy season for Dire Dawa. The wind occasionally covers the city in the form of a dust storm, increasing the number of dust particles in the atmosphere, while the rain does the reverse (cleaning the atmosphere). The increment is, however, attributed to the increasing trend of wind over recent years, especially from the eastern side of the city, carrying with it dust particles picked from arid areas.

The seasonality of AOD is evident and can be connected to the frequent sandstorms that occur in the early spring, as reported by Li et al. (2021). Che et al. (2012) observed minimum AOD concentration in winter. The average AOD during the rainy season (spring and summer) is the largest, according to an analysis of seasonal fluctuations in the four

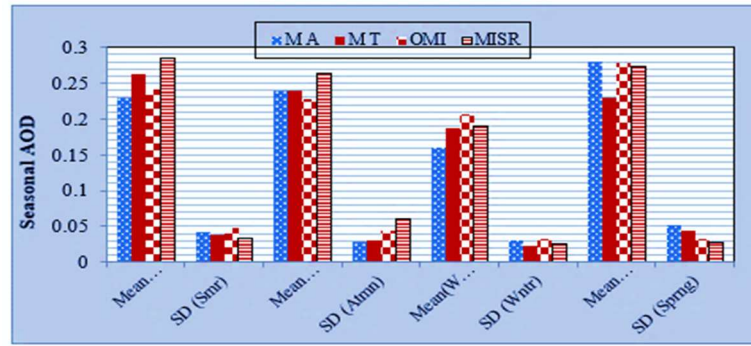


Fig. 6: Twelve-year mean and standard deviations of AOD of the four seasons shown for the four sensors.

Table 4: The summary of AOD trend analysis using the M.K. test and Sen's slope estimator in Dire Dawa from 2009 to 2020.

Sensor	Period	P	Mann-Kendall trend test parameters				Decision
			Z	Tau(τ)	Sen's slope		
MODIS-Aqua	Annual		0.019	2.337	0.530	0.008	Trend(increasing)
	Season	Summer	0.024	2.263	0.515	0.007	Trend (increasing)
		Autumn	0.011	2.537	0.576	0.006	Trend(increasing)
		Winter	0.271	1.100	0.258	0.001	No trend
		Spring	0.007	2.674	0.606	0.013	Trend(increasing)
MODIS-Terra	Annual		0.115	1.577	0.364	0.006	No trend
	Season	Summer	0.064	2.537	0.576	1.851	No trend
		Autumn	0.011	2.537	0.576	0.0 059	No trend
		Winter	0.732	0.343	0.091	0.00 075	No trend
	Spring	0.086	1.714	0.394	0.0063	Trend(increasing)	
MISR	Annual		0.754	-0.003	-0.313	-0.111	No trend
	Season	Summer	0.602	-0.521	-0.167	-0.001	No trend
		Autumn	0.917	0.104	0.056	0.003	No trend
		Winter	0.754	-0.313	-0.111	-0.003	No trend
	Spring	0.251	1.147	0.333	0.006	No trend	
OMI	Annual		0.115	0.005	1.577	0.005	No trend
	Season	Summer	0.054	1.925	0.439	0.006	No trend
		Autumn	0.451	0.754	0.182	0.004	No trend
		Winter	0.837	0.206	0.061	0.002	No trend
	Spring	0.039	2.062	0.470	0.004	Trend(increasing)	

periods. This is likely because updrafts emerge as local surfaces warm up. In addition, wind speeds hasten the movement of mobile dunes; the accumulation of upward air and related dust on natural surfaces results in the highest AOD concentrations in the wet season, and low AOD values in winter are due to fewer sandstorms, snowfall, and decreased winter wind and dust activity (Li et al. 2021, Humera et al. 2017). The high AOD in summer is associated with coarse particles, and the lower AOD in Winter is associated with fine particles. The winter season shows low AOD values due to the presence of

clouds, so aerosols act as a cloud condensation nucleus along with low wind speed, and therefore, the amount of aerosol dust reduction leads to low AOD values. As reported by Asmarech & Jaya (2021), the main cause of AOD in the winter due to large emissions of smoke and soot due to biomass burning. Biomass burning is also a frequent source of atmospheric pollution and poor air quality (Li et al. 2015).

Even though there are no remarkable differences in AOD among the seasons, the spring season exhibited the highest (0.20 - 0.35) and winter the lowest (0.15 - 0.22). Summer

and autumn had similar AOD concentrations of 0.20 - 0.29 (Fig. 6). As shown in Fig. 6, in terms of seasonal mean OMI recorded (0.284 ± 0.034) in the summer season > MODIS-Aqua (0.28 ± 0.051) observed in spring season > MISR (0.278 ± 0.033) recorded in spring season > MODIS-Terra (0.262 ± 0.039) observed in the summer season. On the other hand, the maximum AOD value was observed in the spring season (0.352) from MODIS-Aqua, and the minimum AOD value was obtained in the winter season (0.011) with the MISR sensor. The study revealed that the AOD values in spring and summer are significantly higher than those in autumn and winter.

During the wet season, due to a higher temperature, soil moisture is evaporated, and heated soil due to high wind velocities, which can increase AOD values, and a higher concentration of water vapors leads to a higher AOD (Alam et al. 2014; Filonchik et al. 2019). High temperature and humidity are favorable conditions that increase gas to the particle conversion process and the hygroscopic growth of aerosol. In contrast, the low value of AOD in the dry season, particularly the winter season, is caused by the low surface temperature, which results in the weak production of mineral dust derived from the soil surface (Li et al. 2015).

Trend Analysis of AOD Using the Mann-Kendall Trend Test

The M.K. analysis shown in Table 4 is calculated for annual

and seasonal AOD trends at a significant level of 0.05 for all four sensors.

As shown in Table 4, by comparing the P-value with alpha (5%). When the P-value is less than 0.05, there is a significant positive AOD trend.

Based on this test, only MODIS-Aqua showed a positive increasing trend in the annual period and during the summer, autumn, and spring seasons. From Sen's slope, the annual magnitude is 0.008 y^{-1} and 0.007, 0.006, and 0.013 per year for the three seasons, respectively. Aside from MODIS aqua, MODIS-terra and OMI showed increasing trends with Sen's slopes of 0.006 and 0.004, respectively. Similarly, the study of Arfan et al. (2017) revealed that the increasing AOD trends (95% statistical significance) are evident in spring (0.009 y^{-1}), summer (0.019 y^{-1}), and autumn (0.005 y^{-1}), but not in winter (0.003 y^{-1}). As shown in Table 4 above, it is observed that increasing AOD trend values were observed during the wet season (spring and summer), and this is due to the increase in convective activities that enhance wind speed and surface temperature. The speed of wind initiated and facilitated the movement of copious amounts of soil dust aerosols into the atmosphere from the surface of dry ground of the arid and semi-arid regions, as reported by Asmarech & Jaya (2021) in their study on AOD over selected areas of Northern Ethiopia. The study of Oluwasinaayomi et al. (2018) revealed that in Dire

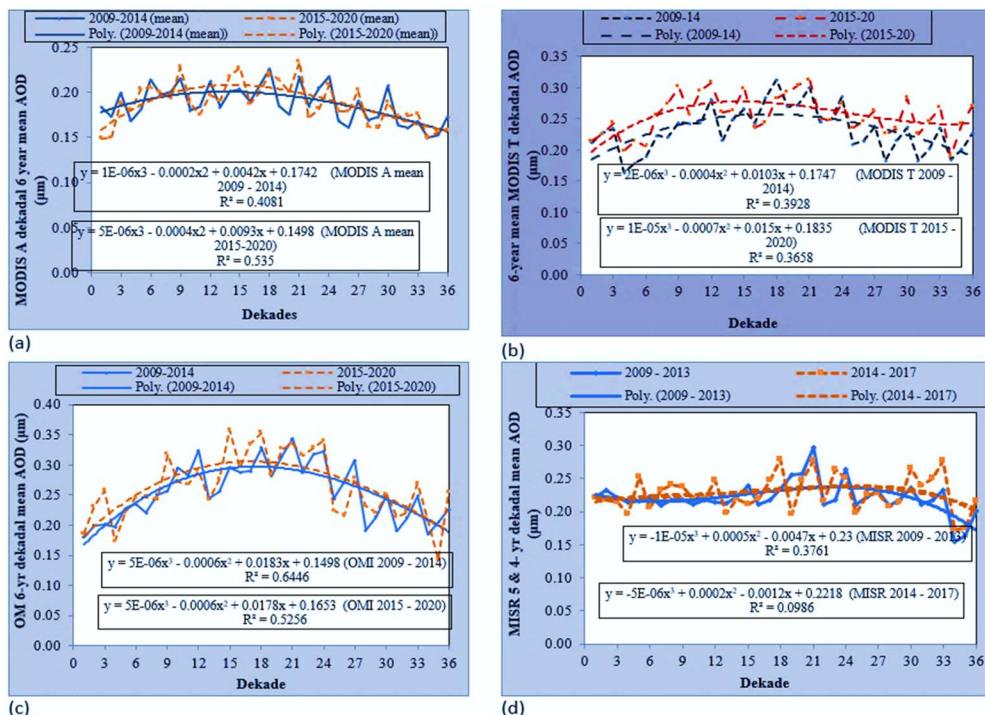


Fig. 7: AOD means decadal distribution retrieved using (a) MODIS-Aqua, (b) MODIS-Terra, (c) MISR (d) OMI from 2009 to 2020 over Dire Dawa.

Table 5: Mean monthly and standard deviation from 2009 to 2020 over Dire Dawa.

Sensor	Monthly mean AOD values											
	Sept.	Oct.	Nov.	Dec.	Jan.	Feb.	March	April	May	June	July	Aug.
MODIS-A	0.259±0.05	0.226±0.04	0.212±0.05	0.158±0.05	0.134±0.03	0.183±0.03	0.28±0.05	0.28±0.06	0.277±0.05	0.245±0.07	0.291±0.05	0.297±0.05
MODIS-T	0.253±0.03	0.233±0.04	0.234±0.03	0.234±0.03	0.14±0.03	0.188±0.03	0.224±0.04	0.248±0.04	0.218±0.04	0.26±0.04	0.262±0.04	0.265±0.04
OMI	0.277±0.04	0.279±0.06	0.235±0.09	0.212±0.04	0.144±0.03	0.219±0.05	0.263±0.04	0.283±0.03	0.273±0.03	0.273±0.04	0.293±0.05	0.285±0.03
MISR	0.219±0.06	0.224±0.04	0.236±0.05	0.18±0.04	0.222±0.05	0.218±0.05	0.305±0.02	0.300±0.05	0.217±0.05	0.241±0.07	0.257±0.04	0.247±0.06

Dawa, the poor air quality outcomes are further compounded by rural-urban migration, increasing population, poor land use planning and management, poverty, soil degradation, loss of vegetation cover, expansion of informal settlement, and inadequate waste management system.

Dekadal Trend of AOD over Dire Dawa from 2009 to 2020

At first, an attempt was made to see the variability of AOD every ten days throughout 2009 – 2020. Then, we found that trends were identical for 2009–2014 and 2015 –2020. Thus, we divided the period into two parts and analyzed the trends as shown in Fig. 4a – 4d. In the first period (2009-2014), MISR data from 2009-2013 were included. During the second period (2015 to 2020), MISR data was incomplete and thus excluded.

The 12 years were divided into two because there is a kind of cyclic behavior. Since there are three decades in a month, a total of 36 decades were considered for the six years. The plots of the two six years were done on the same axes for curve fitting purposes and to see changes that have taken place over the 12 years. The peaks of both curves occurred around the 18th decade (3rd year). In all four curves, the minimum occurred at the beginning and the end of the 6th year. That means the minimum occurred in 2009, 2015, and 2020. The maximum occurred in 2011 and 2017. The maximum AOD was around 0.21 for MODIS aqua, 0.28 for MODIS terra, 0.30 for OMI, and 0.23 for MISR. OMI and MODIS terra showed a higher range of 0.17 – 0.28, while MODIS aqua and MISR exhibited similar ranges of 0.18 – 0.23. This reveals that the results of all four sensors are close to each other as far as AOD data is concerned.

As illustrated in Fig.7, MODIS-Terra AOD showed an increment from the first 6 years (2009 – 2014) to the second six years (2015 – 2020). This shows changes in Dire Dawa in terms of urbanization, land use/land cover, and climate change, such as an increase in temperature or reduction of rainfall. Such change was not observed with MODIS –Aqua AOD. OMI exhibited a very subdued change. MISR did not clearly show such a change, perhaps due to incomplete data, sensor retrieval performance, and surface reflectance. The cause could be linked to meteorological phenomena such as abundant rainfall (for the low times) and dry periods for the high AOD times. Besides, the sand particles in the desert areas and dust on bare surfaces increase the amount of particulate matter in the atmosphere. On a large scale, this leads to maximum AOD values.

Mean Monthly Distribution of AOD

Mean monthly AOD concentrations were obtained from the daily data. In this study, the mean AOD for the 12 months from 2009 to 2020 was processed in a unified manner, and the

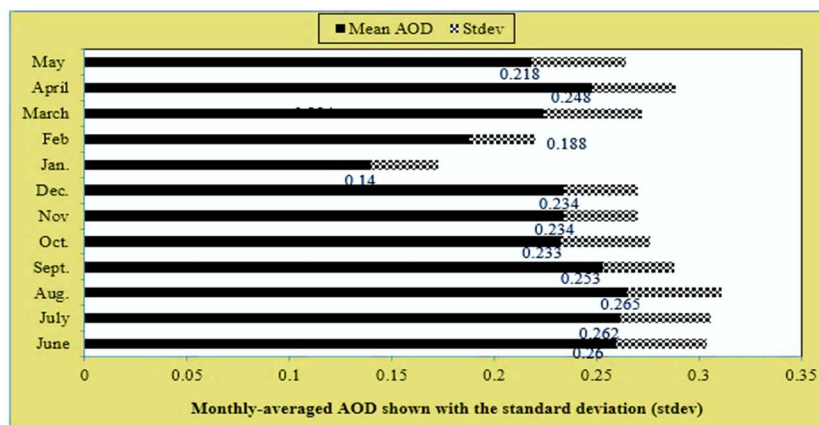


Fig. 8: Monthly-averaged MODIS-terra AOD of Dire Dawa for 2009 -2020 shown with the standard deviation (stdev).

results are shown in Table 5. The result shows that the AOD value retrieved using the MODIS-Aqua, MODIS-Terra, MISR, and OMI ranged from 0.14 to 0.305. As shown in Table 5, the mean monthly AOD was in the range of 0.134 – 0.297 for MODIS-Aqua, 0.14–0.265 for MODIS –Terra, 0.144 – 0.293 for OMI and 0.18 – 0.305 for MISR sensor. Since MODIS-terra represents Dire Dawa AOD better than the other sensors, the monthly-averaged AOD of this sensor is shown for all the months in Fig. 8.

Fig 8 shows that in the spring season (MAM) and summer season (JJA), AOD distribution recorded relatively higher values than the rest of the months. September, April, and August months exhibited higher AODs, while January exhibited the least. The variability within each month seems to be proportional to the mean AOD itself since the standard deviations were higher when mean AODs were higher and lower when the mean AODs were lower (e.g., January and February). One possibility why AOD is highest in August has something to do with more water vapor in the atmosphere, which is to be expected since these are the times when the dust and black cloud events occur in the region. Since aerosol particles serve as nucleation centers for condensation, the more the condensation, the more the aerosol particles are trapped in water vapors.

On the contrary, in January, there is very low water vapor in the atmosphere, resulting in less AOD. The monthly mean values of (MODIS) aerosol optical depth (AOD) at 550 nm examined by Marey et al. (2011) on aerosol climatology over the Nile Delta based on MODIS, MISR, and OMI sensors showed significant monthly variability of AOD to be maximum in April or May (~0.5) and a minimum in December and January (~0.2). Similarly, in the study made by Asmarech and Jaya (2021), the monthly mean seasonal variations of AOD show a maximum value in (June, July, and August). A minimum value in (December, January, and

February) in their study on AOD variability over the Northern part of Ethiopia and Djibouti using MODIS sensor. The study further revealed that the aerosol distribution over Ethiopia is highly variable spatially and temporally.

CONCLUSIONS

The comparison of AOD with AERONET indicated that all three sensors showed a positive linear correlation with AERONET data, but MODIS-Terra exhibited the best representation. The inter-comparisons of AOD retrieved from multi-spectral satellite sensor show that the linear curve with intercept, none (except the fit between MODIS Terra and OMI) gave even satisfactory correlations as seen from the R^2 values. From the linear curve fit without intercept, MODIS-Aqua and MISR AOD revealed better correlations. This cross-comparison of several sensors is occasionally required since bias and mistakes in retrieval methods are present because of instrument calibration, sampling, and algorithm correctness.

Out of the annual trends of the four sensors, only the one with MODIS-aqua showed a satisfactory increasing linear trend. Season-wise, MODIS-aqua and OMI exhibited satisfactory increasing linear trends in summer, autumn, and spring. No trend was observed in winter. This shows that the seasonal data give better information about the AOD trend of the area than the annual. The three seasons exhibited almost similar AOD values, while the winter season showed the least. The month of lowest AOD was January, whereas August was the highest, and there seems to be a link between AOD and the amount of water vapor in the atmosphere. As far as decadal AOD is concerned, MODIS-terra (which best represents AOD over Dire Dawa) revealed the difference between the years 2009-2014 and 2015-2020 (increasing trend). Overall, the study shows an increasing AOD trend over Dire Dawa during the 12 years (2009 - 2020). This study

further concludes that MODIS-Terra can be a suitable sensor for AOD data retrieval over bright surfaces & semi-arid areas in Dire Dawa, Ethiopia. The AOD values were observed to be higher in summer (June to August) than during the rest of the months due to the predominance of coarse dust and sea salt particles and possibly also due to the higher water vapor content of the atmosphere due to high summer temperatures, which encourages the growth of aerosols.

Additionally, it was observed that significant AOD levels occurred in October, which may be related to crop harvesting and the ensuing plumes from biomass burning. From January through April, the AOD rises, then falls until December, and April is the month with the highest AOD. The springtime and summertime dust aerosols might be associated with the major contributors to AOD variations in addition to high meteorological parameters variability (wind speed, temperature, rainfall, relative humidity, etc.) and emissions from biomass burning, vehicles, and factories. This study also revealed that the deterioration of the air environment was more prominent and severe. The study's findings are significant in that they serve as a guide for satellite retrieval end users on which airborne over a specific geographic area and AOD range, sensors might offer accurate data. Satellite data such as MODIS, MISR, and OMI provide useful complementary information to investigate the optical and physical characteristics of aerosol.

The AOD collected over Dire Dawa showed notable discrepancies in aerosol variations and trends, which may be related to dust emissions, biomass burning, fossil fuel combustion, and socioeconomic practices. By lowering the burden of disease linked to air pollution and assisting in the short and long-term mitigation of climate change, policies to reduce air pollution offer a win-win strategy for both climate and health. In the past, satellite remote sensing of air quality was largely limited to monitoring at low temporal resolution (e.g., monthly). Advances in satellite sensors and modeling techniques enable shifts in research direction toward operational monitoring and forecasts of air quality and incorporation of multiple data sources to improve monitoring and forecast skills. These efforts will, consequently, improve our responses to public health problems and broader intercountry issues on air pollution. Moreover, this provides tangible information that can be helpful for policymakers, urban air quality monitors, communities, researchers, and all other stakeholders concerned with preventing and monitoring air quality. Therefore, these studies have important implications for climate systems and take a mitigation approach to monitor air quality over urban regions.

Further work is required to quantitatively understand the contributing factors from a natural and anthropogenic source

responsible for AOD variability so that regulations can target specific factors of high priority/importance. These studies also provide us with more specific information about the functionality of particular sensors at the local and regional levels. The study also strongly recommends making use of a synergy of remote sensing and ground-installed devices, such as sun photometers, to monitor the status of air quality on a daily, decadal, monthly, annual, and seasonal basis over polluted urban areas.

ACKNOWLEDGMENT

We would also like to express our gratitude to NASA for providing MODIS, MISR, and OMI aerosol products, all of which are available from the GES DISC at NASA Goddard. Finally, the authors would like to express their sincere gratitude to the Center of Environmental Sciences at Addis Abeba University for providing the remote sensing equipment and training that helped to better complete this study.

REFERENCES

- Ahn, C.O., Torres, O. and Jethva, H. 2014. Assessment of OMI near-UV aerosol optical depth over land. *J. Geophys. Res. Atmos.*, 119: 2457-2473. doi:10.1002/2013JD020188.
- Alam, K., Khan, R., Ali, S., Ajmal, M., Khan, G., Muhammad, W. and Ali, M. 2014. Variability of aerosol optical depth over Swat in Northern Pakistan based on satellite data. *Arab. J. Geosci.*, 8(1): 547-555.
- Ashraf, F. 2019. Comparative analysis of MODIS, MISR, and AERONET climatology over the Middle East and North Africa. *Ann. Geophys.*, 37: 49-64. <https://doi.org/10.5194/angeo-37-49>.
- Ashraf, F. 2018. Comparative analysis of MODIS, MISR, and AERONET climatology over the Middle East and North Africa. *Ann. Geophys. Discuss.*, 1: 79. <https://doi.org/10.5194/angeo-2018-79>
- Asmarech, E. and Jaya, P.R. 2021. Daily and seasonal variation of aerosol optical depth and angstrom exponent over Ethiopia using MODIS Data. *Pollution*, 8(1): 315-329. DOI: 10.22059/POLL.2021.316010.971.
- Badarinath, K.V.S. Goto, D., Kharol, S.K., Mahalakshmi, D.V., Sharma, A.R. and Nakajima, T. 2011. Influence of natural and anthropogenic emissions on aerosol optical properties over a tropical urban site. *Atmos. Res.*, 100: 111-120. <https://doi.org/10.1016/j.atmosres.2011.01.003>.
- Belachew, M. and Zeleke, D.A. 2015. Statistical analysis of road traffic car accident in Dire Dawa Administrative City, Eastern Ethiopia. *Sci. J. Appl. Math. Stat.*, 3(6): 250-256.
- Bibi, M. 2015. Intercomparison of MODIS, MISR, OMI, and CALIPSO aerosol optical depth retrievals for four locations on the Indo-Gangetic plains and validation against AERONET data. *Atmos. Environ.*, 111: 113-126.
- Che H., Wang Y., Sun J. Zhang X., Zhang X. and Guo J. 2012. Variation of aerosol optical properties over Taklimakan Desert of China. *Aerosol and Air Quality Research*, 13(2): 777-785. DOI 10.4209/aaqr.2012.07.0200.
- Cheng, T., Chen, H., Gu, X., Yu, T., Guo, J. and Guo, H. 2012. The inter-comparison of MODIS, MISR, and GOCART aerosol products against AERONET data over China. *J. Quant. Spectrosc. Radiat. Transf.*, 113: 2135-2145. <http://dx.doi.org/10.1016/j.jqsrt.2012.06.016>.
- Eck, T.F., Holben, B.N., Reid, J.S., Sinyuk, A., Dubovik, O., Smirnov, A., Giles, D., O'Neill, N.T., Tsay, S.C., Ji, Q., Al Mandoos, A., Ramzan Khan, M., Reid, E.A., Schafer, J.S., Sorokine, M., Newcomb, W.

- and Slutsker, I. 2008. Spatial and temporal variability of column-integrated aerosol optical properties in the southern Arabian Gulf and United Arab Emirates in summer. *J. Geophys. Res.*, 113: 01204. doi:10.1029/2007JD008944.
- Filonchik, M., Yan, H., Zhang, Z., Yang, S., Li, W. and Li, Y. 2019. Combined use of satellite and surface observations to study aerosol optical depth in different regions of China. *Sci. Rep.*, 9: 66-74. http://doi.org/10.1038/s41598-019-42466-6.
- Floutsi, A.A., Korras-Carraca, M.B., Matsoukas, C., Hatzianastassiou, N., Biskos, G. 2016. Climatology and trends of aerosol optical depth over the Mediterranean basin during the last 12 years (2002-2014) based on Collection 006 MODIS-Aqua data. *Science of The Total Environment*, 551-552: 292303. doi:10.1016/j.scitotenv.2016.01.192
- Ge, J.M., Huang, J.P., Su, J., Bi, J.R. and Fu, Q. 2011. Short wave radiative closure experiment and direct forcing of dust aerosol over northwestern China. *Geophys. Res. Lett.*, 38: 4975. https://doi.org/10.1029/2011GL049571
- Gezahegn, B. T., Elias, F.M. and Aklile, A.E. 2021. Trends in daily temperature and precipitation extremes over Dire-Dawa, 1980-2018. *J. Environ. Earth Sci.*, 11(9): 45-76.
- Gupta P., Lorraine A., Remer, Robert C., Levy, and Shana M. 2018. Validation of MODIS 3 km land aerosol optical depth from NASA's EOS Terra and Aqua missions. *Atmos. Meas. Tech.*, 11: 31453159. https://doi.org/10.5194/amt-11-3145-2018
- Holben, B., Eck, T., Slutsker, I., Tanré, D., Buis, J., Setzer, A., Vermote, E., Reagan, J., Kaufman, Y., Nakajima, T., Lavenu, F., Jankowiak, I. and Smirnov, A. 1998. AERONET – A federated instrument network and data archive for aerosol characterization. *Remote Sens. Environ.*, 66: 1-16.
- Hsu, N.C., Jeong, M.J., Bettenhausen, C., Sayer, A.M., Hansell, R., Sefstor, C.S., Huang, J. and Tsay, S.C. 2013. Enhanced deep blue aerosol retrieval algorithm: The second generation. *J. Geophys. Res. Atmos.*, 118: 9296-9315.
- Humera, B., Khan, A., Farrukh, C., Samina, B., Imran, S. and Thomas, B. 2017. Intercomparison of MODIS, MISR, OMI, and CALIPSO aerosol optical depth retrievals for four locations on the Indo-Gangetic plains and validation against AERONET data. *Atmos. Environ.*, 11: 113-126. http://dx.doi.org/10.1016/j.atmosenv.2015.04.013.
- IPCC. 2013. Contribution of Working Group I to the Fifth 4 Assessment Report of the Intergovernmental Panel on Climate Change. In Stocker, T.F., Qin, D., Plattner, G.K., Tignor, M., Allen, S.K., Boschung, J., Nauels, A., Xia, Y., Bex, V. and Midgley, P.M. (eds), *Climate Change 2013: The Physical Science Basis*, Cambridge University Press, Cambridge, UK and New York, NY, pp. 15324-15335. https://doi.org/10.1017/CBO9781107415324.
- Jung, J., Souri, A.H., Wong, D.C., Lee, S., Jeon, W., Kim, J. and Choi, Y. 2019. The impact of the direct effect of aerosols on meteorology and air quality using aerosol optical depth assimilation during the KORUS AQ campaign. *J. Geophys. Res. Atmos.*, 124: 8303-8319. https://doi.org/10.1029/2019JD030641.
- Kazuhsa, T., Hiroshi, M., Tadaihiro, H. and Mayumi, Y. 2022. Aerosol Optical Properties of Extreme Global Wildfires and Estimated Radiative Forcing with GCOM-C SGLI, Egusphere, https://doi.org/10.5194/egusphere-2022-21.
- Knife, M. 2017. Evaluation of air pollutant levels in Dire-Dawa City, Ethiopia. *Int. J. Environ. Sci. Nat. Resour.*, 7(3): 555711.
- Kristjánsson, J.E., Muri, H., Boucher, O., Huneus, N., Kravitz, B. and Robock, A. 2014. *J. Geophys. Res. Atmos.*, 119: 1-17. http://dx.doi.org/10.1002/2013JD021060.
- Levelt, P.F., Hilsenrath, E., Leppelmeier, G.W., van den Oord, G.H.J., Bhartia, P.K., Tamminen, J., de Haan, J.F. and Veefkind, J.P. 2006. Science objectives of the ozone monitoring instrument. *IEEE Trans. Geosci. Remote Sens.*, 44(5): 1093-1101.
- Levy, R.C., Remer, L.A., Kleidman, R.G., Mattoo, S., Ichoku, C., Kahn, R. and Eck, T.R. 2010. Global evaluation of the collection of 5 MODIS dark-target aerosol products over land. *Atmos. Chem. Phys.*, 10: 10399-10420. doi:10.5194/acp-10-10399-201.
- Levy, R.C., Mattoo, S., Munchak, L.A., Remer, L.A., Sayer, A.M., Patadia, F. and Hsu, N.C. 2013. The Collection 6 MODIS aerosol products over Land and ocean. *Atmos. Meas. Tech.*, 6: 2989-3034. https://doi.org/10.5194/amt-6-2989-2013.
- Li, J., Ge, X., He, Q. and Abbas, A. 2021. Aerosol optical depth (AOD): Spatial and temporal variations and association with meteorological covariates in Taklimakan desert, China. *Peer J.*, 9: e10542. DOI 10.7717/peerj.10542.
- Li, S., Wang, T., Xie, M., Han, Y. and Zhuang, B. 2015. Observed aerosol optical depth and angstrom exponent in the urban area of Nanjing, China. *J. Atmos. Environ.*, 123: 350-356.
- Marey, H.S., Gille, J.C., El-Askary, H.M., Shalaby, E.A. and El-Raey, M.E. 2011. Aerosol climatology over the Nile Delta based on MODIS, MISR, and OMI satellite data. *Atmos. Chem. Phys.*, 11: 10637-10648. doi:10.5194/acp-11-10637.
- Martonchik, J.V., Diner, D.J., Kahn, R.A., Ackerman, T.P., Verstraete, M.M., Pinty, B. and Gordon, H.R. 2002. Techniques for the retrieval of aerosol properties over land and ocean using multiangle imaging. *Geosci. Remote Sens. IEEE Trans.*, 36: 1212-1227.
- Mengistu, A. and Amente, M. 2020. Reformulating and testing Temesgen: Melesse's temperature-based evapotranspiration estimation method. *Heliyon*, 6: 02954. https://doi.org/10.1016/j.heliyon.2019.e02954.
- Oluwasinaayomi, F.K., Mulneh, W., Abshare, M. and Samuel Babatunde, A. 2018. Analysis of air quality in Dire Dawa, Ethiopia. *J. Air Waste Manag. Assoc.*, 68(8): 801-811. https://doi.org/10.1080/10962247.2017.1413020.
- Ramachandran, M. and Sumita, G. 2013. Aerosol optical properties over South Asia from ground-based observations and remote sensing: A review. *Climate*, 1: 84-119; doi:10.3390/cli1030084 Open Access.
- Ramanathan, V., Crutzen, P. J., Kiehl, T. and Rosenfeld, D. 2001. Aerosols, climate, and the hydrologic cycle. *Science*, 294: 2119-2124.
- Remer, L.A., Kaufman, Y.J., Tanré, D., Mattoo, S., Chu, D.A., Martins, J.V., Li, R.R., Ichoku, C., Levy, R.C., Kleidman, R.G., Eck, T.F., Vermote, E. and Holben, B.N. 2005. The MODIS aerosol algorithm, products, and validation. *J. Atmos. Sci.*, 62: 947-973. http://dx.doi.org/10.1175/JAS3385.1.
- Rosenfeld, D., Dai, J., Yu, X., Yao, Z., Xu, X., Yang, X. and Du, C. 2007. Inverse relations between amounts of air pollution and orographic precipitation. *Science*, 315: 1396. https://doi.org/10.1126/science.1137949 PMID:17347436.
- Taotao, C., Guimin, X., Lloyd, T. Wilson, W. and Daocai, C. 2016. Trend and cycle analysis of annual and seasonal precipitation in Liaoning, China. *Adv. Meteorol.*, 70: 563. http://dx.doi.org/10.1155/2016/5170563.
- Tripathi, S. N., Dey, S., Chandel, A., Srivastava, S., Singh, R. P., and Holben, B. N. 2005. Comparison of MODIS and AERONET derived aerosol optical depth over the Ganga Basin, India, *Ann. Geophys.*, 23: 10931101. https://doi.org/10.5194/angeo-23-1093-2005.
- Wang, S., Cohen, J.B., Lin, C. and Deng, W. 2020. Constraining the relationships between aerosol height, aerosol optical depth, and total column trace gas measurements using remote sensing and models. *Atmos. Chem. Phys.*, 20(23): 15401-15426. https://doi.org/10.5194/acp-20-15401.
- Weizhi, D., Jason Blake, C., Shuo, W. and Chuyong, L. 2021. Improving the understanding between climate variability and observed extremes of global NO₂ over the past 15 years. *Environ. Res. Lett.*, 16(5): 054020. https://doi.org/10.1088/1748-9326/abd502.

ORCID DETAILS OF THE AUTHORS

Teshager Argaw Endale: <https://orcid.org/0000-0003-0117-358X>